Theor Chim Acta (1994) 87: 431–439

Theoretica Chimica Acta

Electronic structure and the hydrogen-shift isomerization of hydrogen nitryl HNO_2

Shin-ya Takane and Takayuki Fueno

Department of Chemistry, Faculty of Engineering Science, Osaka University, Toyonaka, Osaka 560, Japan

Received November 19, 1992/Accepted June 30, 1993

Summary. Electronic structure of hydrogen nitryl HNO_2, a yet not identified entity, and the path of its possible isomerization to *trans*-HONO have been investigated by *ab initio* SCF and MRD-CI computations using the 6-31G** basis set. HNO_2 is C_{2v}-symmetric and its ground state ($^1A_1$) is less stable than *trans*-HONO by 66 kJ/mol (with the SCF vibrational zero-point energy correction). The lowest two excited singlet states ($^1A_2$ and $^1B_1$) are nearly degenerate, their vertical excitation energies being predicted to be 4.8 eV. The isomerization path is traced by the CASSCF procedure and the activation barrier height is evaluated by the CI treatment. HNO_2 in its ground state isomerizes to *trans*-HONO by maintaining the planar (C_s-symmetric) structure. The activation energy is calculated to be 171 kJ/mol, which is clearly lower than the calculated H–N bond energy (253 kJ/mol). The transition state seems to be more adequately described as an interacting system of proton and the nitrite anion rather than as a pair of two fragment radicals.

Key words: Hydrogen nitryl (HNO_2) – Nitro compound – Hydrogen migration – Isomerization

1 Introduction

In our previous work [1], we investigated the gas-phase reaction of NH with O_2 by the *ab initio* method. It was found that the reaction between $NH(^3\Sigma^-)$ and $O_2(^3\Sigma_g^-)$ should proceed by an initial association giving a chain intermediate $HNOO(^1A')$:

$$NH(^3\Sigma^-) + O_2(^3\Sigma_g^-) \rightarrow HNOO \tag{1}$$

By contrast, the reaction between $NH(^1\Delta)$ and $O_2(^1\Delta_g)$ should be a concerted cycloaddition to give a cyclic HNO_2. It will easily isomerize into nitrous acid

HONO via an acyclic HNO_2 (**1**) of the C_{2v} symmetry [2]:

$$NH(^1\Delta) + O_2(^1\Delta_g) \rightarrow \underset{\mathbf{1}}{\text{H–N}\begin{smallmatrix}\diagup\text{O}\\ \\ \diagdown\text{O}\end{smallmatrix}} \rightarrow \text{H–N}\begin{smallmatrix}\diagup\text{O}\\ \\ \diagdown\text{O}\end{smallmatrix} \tag{2}$$

$$\underset{\mathbf{1}}{} \rightarrow \underset{\mathbf{2}}{\text{HONO}} \tag{3}$$

The singlet species **1**, which we here refer to as hydrogen nitryl, is the branched isomer of nitrous acid **2** and should be the simplest possible nitro compound. It has never been identified experimentally so far. The challenge to identify this isomer was first made by Jones et al. [3], who observed no indication of its contribution in the IR spectra of gaseous nitrous acid. It could also be one of the transient intermediates of the well-known gas-phase reaction of the H atom with NO_2 to produce the NO and OH radicals [4–8]. Guillory et al. [9] carried out IR spectroscopic studies of the products of the H + NO_2 reaction conducted by the matrix isolation technique, to observe *cis*- and *trans*-HONO alone; no trace of the nitro form (**1**) was discernible.

Hydrogen nitryl (**1**) may be used as a convenient prototype for existing nitro compounds in assessing their thermochemical stabilities relative to the chain isomers [10]. To the best of our knowledge, however, there has been no explicit study to trace the path of its isomerization pathway (Eq. (3)). Elucidation of the intrinsic path of Eq. (3) by *ab initio* SCF and CI calculations is the primary concern of the present investigation. We will also attempt theoretical predictions of the vertical singlet excitation energies of **1**.

2 Method of calculations

The path of isomerization was traced first by the RHF SCF procedure, using the Gaussian 86 program package [11]. The atomic orbital functions used in this study are primarily the 6-31G** basis set [12] throughout, unless otherwise stated. The transition state (TS) was located and verified by the vibrational analysis. For all the stationary points on the isomerization path (i.e., HNO_2, TS, and *trans*-HONO), CASSCF (8 electrons in 6 orbitals) calculations by the use of the HONDO program [13] were then performed to improve their geometries. For the fragment radicals, the unrestricted Hartree-Fock (UHF) method was used.

At all the optimized geometries, multi-reference double-excitation configuration-interaction (MRD-CI) calculations were carried out. The Table CI program [14, 15] furnished by Buenker was used. The configuration-selection and extrapolation routines were followed [16]. The maximal dimension of the configuration space used was 8000–10,000. The extrapolated CI energies were all subjected to the Langhoff-Davidson corrections [17], to estimate the full CI limit values E_{CI}. To determine the reference (main) configurations, we preliminarily performed a single-reference SD-CI calculation at each state. The configurations whose contributions $|C_i|^2$ to a state under consideration exceeded 0.3% were then regarded as the reference configurations. In this manner, the total number of the reference configurations adopted were typically 3 to 5, and the total sum of the weights $|C_i|^2$ of the reference configurations were at least 0.90.

In calculating the vertical excitation energies, the lowest three roots (eigenvalues) of the CI matrix for each irreducible representation were evaluated in a similar manner as above. The total number of the reference configurations ranged from 12 to 22 in these multi-root calculations.

3 Results

3.1 Electronic structure

The C_{2v} geometry for hydrogen nitryl (**1**) optimized at the RHF level is shown in Fig. 1a. The reference configurations adopted in the subsequent CI calculation are shown in Table 1, together with their contribution weights (squared weights, $|C_i|^2$).

As can be seen in Table 1, the contribution of the electronic configuration:

$$A_1;\ (1a_1)^2 \cdots (1b_1)^2(4b_2)^2(6a_1)^2(1a_2)^2$$

to the ground state of HNO_2 (**1**) amounts to 0.87. The contribution of a configuration arising from the transition $(1a_2)^2 \rightarrow (2b_1)^2$ (i.e., the $\pi \rightarrow \pi^*$ double excitation) is as large as 0.025. The result clearly indicates the necessity of a multi-configurational treatment for a more adequate representation of the ground state geometry.

Under such circumstances, the CASSCF (8-6, i.e., eight active electrons distributed in six orbitals) method was used to further optimize the geometry. The result is shown in Fig. 1b. It can be seen that the N–O bond length obtained at the CASSCF method is considerably longer than that at the RHF SCF level, while the remaining parameters are little altered.

At the CASSCF optimized geometry, several vertical singlet excitation energies of HNO_2 were evaluated by the multi-root CI calculations. The basis sets used there were the 6-31G** functions augmented with a single primitive Rydberg *s*-type function ($\xi = 0.028$) on the N atom. All the molecular orbitals used for these calculations were those of the ground-state HNO_2 consistently. The dominant

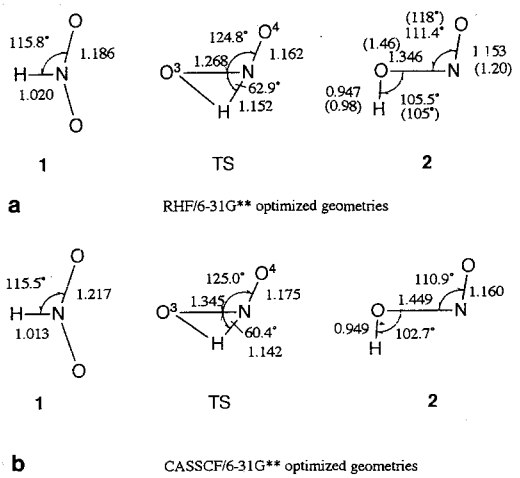

Fig. 1. Geometries of hydrogen nitryl (**1**), the transition state (TS) and *trans*-HONO (**2**) optimized by (**a**) the RHF/6-31G** and (**b**) the CASSCF/6-31G** procedures. The bond lengths are given in units of Å. Given in parentheses are the experimental geometric data [19]

Table 1. The reference configurations used in the CI calculations and their weights[a]

	Configurations	$\|C_i\|^2$
HNO_2 (**1**)		
	$\ldots(1b_1)^2(4b_2)^2(6a_1)^2(1a_2)^2$	0.8681
	$(1b_1)^2 \rightarrow (2b_1)^2$	0.0037
	$(1a_2)^2 \rightarrow (2b_1)^2$	0.0249
	$(1b_1) \rightarrow (2b_1)$	0.0039
TS		
	$\ldots(2a'')^2(10a')^2$	0.8722
	$(2a'')^2 \rightarrow (3a'')^2$	0.0144
	$(1a'')^2 \rightarrow (3a'')^2$	0.0042
	$(1a'') \rightarrow (3a'')$	0.0040
	$(2a'') \rightarrow (3a'')$ $(10a') \rightarrow (13a')$	0.0030
trans-HONO (**2**)		
	$\ldots(10a')^2(2a'')^2$	0.8878
	$(1a'')^2 \rightarrow (2a'')^2$	0.0076
	$(1a'')^2 \rightarrow (3a'')^2$	0.0039
	$(10a') \rightarrow (12a')$ $(2a'') \rightarrow (3a'')$	0.0036
	$(1a'') \rightarrow (3a'')$ $(2a'') \rightarrow (3a'')$	0.0035

[a] The MRD-CI calculations were carried out at the RHF SCF optimized geometries shown in Fig. 1a

electron configurations for the lowest-lying excited states that belong to different irreducible representations of the C_{2v} point group are all such that accommodate an electron in the $2b_1$ orbital:

$$B_1; \cdots (1b_1)^2(4b_2)^2(6a_1)^1(1a_2)^2(2b_1)^1 \qquad (6a_1) \rightarrow (2b_1)$$

$$B_2; \cdots (1b_1)^2(4b_2)^2(6a_1)^2(1a_2)^1(2b_1)^1 \qquad (1a_2) \rightarrow (2b_1)$$

$$A_2; \cdots (1b_1)^2(4b_2)^1(6a_1)^2(1a_2)^2(2b_1)^1 \qquad (4b_2) \rightarrow (2b_1)$$

The vertical excitation energies ΔE_{CI}^{vert} calculated for a few excited states belonging to each irreducible representation are collected in Table 2. For the sake of comparison, the ΔE_{CI}^{vert} values calculated for O_3 and SO_2 [18] as isoelectronic homologs are included in Table 2.

As is shown in Table 2, the lowest excited singlet states are $1A_2$ and $1B_1$, whose vertical excitation energies are both 4.8 eV (the difference being less than 10^{-2} eV) at the CASSCF geometries. The trend is qualitatively similar to the case of ozone, where the vertical excitation energies are 2.2 and 2.3 eV, respectively [18]. The third-lowest excited state is calculated to be the $1B_2$ state (7.5 eV), a result which is in line with the case of SO_2. In the case of O_3, the third-lowest is the $2A_1$ state (4.5 eV), which arises from the double transition $(4b_2)^2 \rightarrow (2b_1)^2$ and hence accommodates a total of six electrons in its π-orbitals. Stability of this 6π-electronic A_1 structure has a bearing with the relatively high stability of the ring isomer of O_3 [18]. As for HNO_2, the second and the third lowest A_1 states, being nearly degenerate (10.5 and 10.6 eV), remain to correspond to 4π-electronic structures.

Table 2. Comparisons of the vertical excitation energies ΔE_{CI}^{vert} of HNO_2, O_2 and SO_2

	ΔE_{CI}^{vert}(eV)		
	HNO_2^a	O_3^b	SO_2^b
$^1A_1$			
1 (ground-state)	(0)	(0)	(0)
2	10.6	4.5	8.7
3	10.5	6.7	9.0
$^1A_2$			
1	4.8	2.2	4.9
2	10.3	6.4	8.5
3	12.0		
$^1B_1$			
1	4.8	2.3	4.5
2	11.4	7.2	8.3
3	13.2		
$^1B_2$			
1	7.5	5.1	6.7
2	10.8	6.8	9.8
3	12.3		

[a] At the CASSCF(8,6)/6-31G** optimized geometry of the ground-state HNO_2
[b] At the MRD-CI optimized geometries [18]

The two excited A_1 states for SO_2 are also nearly degenerate (8.7 and 9.0 eV). The general pattern of electronic excitations for HNO_2 thus resembles more closely that for SO_2 rather than for O_3.

3.2 Isomerization path

The RHF SCF and CASSCF optimized geometries of the transition state (TS) for the isomerization of HNO_2 (**1**) to *trans*-HONO (**2**) are shown in Fig. 1, together with the geometries optimized for *trans*-HONO. The experimental geometric data [19] for *trans*-HONO are given in parentheses. Clearly, the CASSCF method gives the geometry of *trans*-HONO in better agreement with the experimental structure than does the RHF SCF method.

All the geometries shown in Fig. 1 conform to the planar (C_s) symmetry. It has been confirmed that the transition state TS geometry provides one single imaginary frequency ($2640i$ cm^{-1}) at the RHF/6-31G** level. The RHF activation barrier height obtained was $\Delta E^{\ddagger} = 278$ kJ/mol. At the CASSCF/6-31G** level, little change in geometry has been observed except for the N–O[3] bond length, which is slightly longer than the RHF result. The activation barrier height at this level was calculated to be 269 kJ/mol.

Results of MRD-CI calculations at the CASSCF optimized geometries are summarized in Table 3. The total energies of the fragment radical pairs (i.e., $H + NO_2$ and $NO + OH$) are also listed. In calculating the CI energies for these

Table 3. Results of the SCF and MRD-CI calculations

	E_{SCF} + 204 (hartree)	ΔE_{CAS} (kJ/mol)	E_{CI} + 205 (hartree)	ΔE_{CI} (kJ/mol)	ΔE_0^a (kJ/mol)	$\Delta H^{\circ b}$ (kJ/mol)
H + NO_2	− 0.52176[c]		− 0.03822[d]	354	319	325
HNO_2 (1)	− 0.62110	34	− 0.14385	62	66	
TS	− 0.51539	303	− 0.07241	253	237	
trans-HONO (2)	− 0.64401	(0)	− 0.17263	(0)	(0)	(0)
NO + OH	− 0.62582[c]		− 0.09768[d]	198	175	201

[a] The subscript 0 stands for CI + vib

[b] Taken from the literature [19]

[c] Sum of the UHF energies of the fragment radicals

[d] The energies were calculated for the supermolecule models. See text

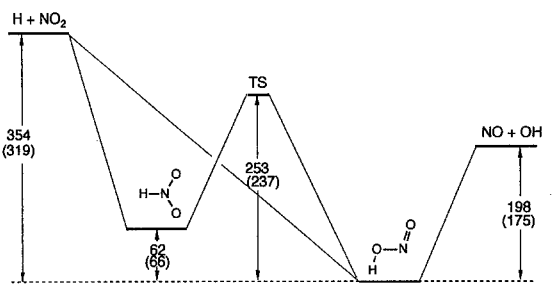

Fig. 2. Potential energy profile (ΔE_{CI}) calculated for the HNO_2-HONO system. Energy gaps shown are in units of kJ/mol. Given in parentheses are the energy differences (ΔE_0) obtained with the vibrational zero-point energy corrections

latter entities, special cautions have been exercised. Thus, in order to minimize the possible size inconsistency in the evaluation of the electron correlation effects, the fragment radical pairs (H + NO_2 and NO + OH) were treated as supermolecules separated by 20.0 Å.

According to the E_{CI} data given in Table 3, HNO_2 (**1**) is less stable than *trans*-HONO (**2**) by 62 kJ/mol. The TS for isomerization lies 253 kJ/mol above **2**. The activation barrier height for the isomerization of **1** to **2** is thus calculated to be $\Delta E_{CI}^{\ddagger} = 191$ kJ/mol. When corrections for the vibrational zero-point energy at the SCF level are included, the relative energy between HNO_2 (**1**) and *trans*-HONO (**2**) comes out to be $\Delta E_0 = 66$ kJ/mol, and the activation energy for the process **1** → **2** is reduced to $\Delta E_0^{\ddagger} = 171$ kJ/mol.

The overall potential energy profile based on the E_{CI} results calculated for the HNO_2-HONO system is diagrammatically shown in Fig. 2. The energy gaps obtained by correcting for the vibrational zero-point energy are given in parentheses. The total CI energies of the H + NO_2 and the NO + OH systems relative to HONO are $\Delta E_{CI} = 354$ and 198 kJ/mol, respectively. Upon corrections for the vibrational zero-point energies, the bond dissociation energies of *trans*-HONO corresponding to the processes:

$$\textit{trans}\text{-HONO} \rightarrow \text{H} + \text{NO}_2 \tag{4}$$

$$\textit{trans}\text{-HONO} \rightarrow \text{NO} + \text{OH} \tag{5}$$

comes out to be $\Delta E_0 = 319$ and 175 kJ/mol, respectively. These results are in reasonable agreement with the respective experimental thermochemical data of

$\Delta H^\circ = 325$ and 201 kJ/mol [19]. The calculated H–N bond energy for HNO_2 is $\Delta E_0 = 253$ kJ/mol.

4 Discussion

As has already been mentioned, the initial step of the reaction between H and NO_2 is a radical association. For this step there can exist two pathways distinct with respect to the position where the H atom attacks NO_2.

$$\mathrm{H} + \mathrm{NO_2} \begin{cases} \longrightarrow \mathrm{HONO}(\textit{trans} \text{ and } \textit{cis}) \\ \longrightarrow \mathrm{HNO_2} \end{cases}$$

One pathway is such that the H atom attacks one of the O atoms of NO_2, thus forming *cis*- or *trans*-HONO, while in the other the H atom attacks the N atom to form the symmetric HNO_2. Guillory et al. [9] have mentioned that since the SOMO of NO_2 is more localized on the N atom as discussed by Walsh [20], the H atom should attack the N atom more favorably than either of the O atoms. However, their experimental results indicated that the HNO_2 (nitro form) did not occur to any significant extent. They concluded that this reaction should proceed through a "hot molecule", HNO_2^*, which would "fly apart" after a short but finite lifetime, or possibly through an activated complex similar in structure to nitrous acid. The results of the present calculations (Fig. 2) indicate that although the isomerization from HNO_2 to *trans*-HONO possesses a large barrier height (171 kJ/mol), it is 82 kJ/mol *lower* than the N–H bond energy (253 kJ/mol) of HNO_2. Thus, the reaction might well proceed to *trans*-HONO via the "hot HNO_2^*". Alternatively, it can be said that HNO_2 is located in a moderately deep well of the potential surface. Therefore, if the hot HNO_2^* could be stabilized effectively, one could well identify or even isolate this intriguing nitro compound.

It is of interest to compare the present results with those for other well-known nitro compounds. On the basis of the MNDO calculations, Dewar and co-workers [21] predicted that the barrier height of the isomerization of nitromethane CH_3NO_2 to methyl nitrite CH_3ONO is $\Delta E^\ddagger = 197$ kJ/mol, which is 61 kJ/mol lower than the energy of the C–N bond rupture. The results were taken as a theoretical justification of the observation by Benson et al. [22], who reported that the thermal decomposition of nitromethane tended to lead to $CH_3O + NO$ in prevalence over $CH_3 + NO_2$. Lee and co-workers [23] estimated the barrier height to be 232 kJ/mol by combining the results of their infrared multiple-photon dissociation (IRMPD) experiments with the RRKM theoretical considerations. The estimated barrier height lend support to the theoretical prediction made by Dewar et al. [21].

On the other hand, recent *ab initio* theoretical studies by McKee based on the CASSCF and MR-CI methods [24] conclude that the isomerization barrier is 42 kJ/mol *higher* than the energy level for $CH_3 + NO_2$. More recently, Saxon and Yoshimine [25] have treated the same unimolecular process by the CASSCF/MR-CI method and concluded that the barrier top lies only marginally *below* the dissociation limit. In addition, Saxon and Yoshimine [26] investigated a similar isomerization of NH_2NO_2 using MCSCF and MR-CI methods, to conclude that the barrier height is only 4 kJ/mol lower than the level for the NH_2 and NO_2

radical pair. All these studies have indicated that the transition states of the isomerization are characterized as interacting fragment radicals placed at a considerably large separation ($\sim$ 3.5 Å).

For HNO_2 which we here deal with, the transition state is not like such radical pairs as in the cases of CH_3NO_2 and NH_2NO_2. As is shown in Fig. 1, little change in the TS geometry is noticeable between the RHF and the CASSCF treatments. Results of the MRD-CI calculations for TS at the RHF optimized geometry (Table 1) provide virtually no indication of the diradical character. The situation remains unaltered when the geometry optimized by the CASSCF/6-31G** procedure was used in the CI calculation. The Mulliken population on the H atom at the TS in the latter calculation is as low as 0.513, a result which indicates the zwitter-ionic character to be represented as $H^+ \ldots NO_2^-$. The trend is in line with the RHF-like character of the TS for the isomerization reaction of HNO_2. Clearly, the H atom as the migrator in the isomerization of HNO_2 is significantly more electropositive as compared to the CH_3 and NH_2 groups relevant to the isomerizations of CH_3NO_2 and NH_2NO_2, respectively. Probably, this difference in electronegativity is a crucial factor governing the distinction between the dynamical mechanisms of the two types (biradical and zwitter-ionic) of the isomerization reactions.

Acknowledgments. This work was supported by the Grant-in-Aid No. 62303002 from the Ministry of Education, Japan. The authors are grateful to Professor R.J. Buenker for supplying the Table MRD-CI program to them. All calculations were carried out on a HITAC M-680H at the Computer Center of the Institute for Molecular Science, Okazaki.

References

1. Fueno T, Yokoyama K, Takane S (1992) Theor Chim Acta 82:299–308
2. Melius CF, Binkley JB (1984) ACS Symp Ser 249: cited in ref. 4
3. Jones LH, Badger RM, Moore GE (1951) J Chem Phys 19:1599–1604
4. Clyne MAA, Thrush BA (1961) Trans Faraday Soc 57:2176–2187
5. McKenzie A, Mulcahy MFR, Steven JR (1974) J Chem Soc Faraday Trans I 70:549–559
6. Spencer JE, Glass GP (1976) Chem Phys 15:35–41
7. Wagner HGg, Welzbacher U, Zellner R (1976) Ber Bunsenges Phys Chem 80:1023–1027
8. Luntz AC (1979) IBM Res Develop 23:596–603
9. Guillory WA, Hunter CE (1971) J Chem Phys 54:598–603
10. Nakamura S, Takahashi M, Okazaki R, Morokuma K (1987) J Am Chem Soc 109:4142–4148
11. Frisch MJ, Binkley JS, Schlegel HB, Raghavachari K, Melius CF, Martin RL, Stewart JJP, Bobrowicz FW, Rohlfing CM, Kahn LR, DeFrees DJ, Seeger R, Whiteside RA, Fox DJ, Fleuder EM, Topiol S, Pople JA (1984) GAUSSIAN 86, Carnegie-Mellon Quantum Chemistry Publishing Unit, Pittsburgh; IMS version registered by Koga N, Yabushita S, Sawabe K, Morokuma K (1990)
12. Hehre WJ, Radom L, Schleyer PvR, Pople JA (1986) *Ab initio* molecular orbital theory. Wiley, NY, p 82
13. Dupuis M, Watts JD, Villar HO, Hurst GJB (1987) HONDO ver. 7.0 QCPE #544, available from Indiana Univ
14. Buenker RJ (1974) Studies in physical and theoretical chemistry, vol 21. Elsevier, Amsterdam, pp 17–34
15. Buenker RJ, Phillips RA (1985) J Mol Struct (TheoChem) 123:291–300
16. Buenker RJ, Peyerimhoff SD (1974) Theor Chim Acta 35:33–58
17. Langhoff SR, Davidson ER (1974) Int J Quant Chem 8:61–72
18. Fueno T, Buenker RJ (1988) Theor Chim Acta 73:123–134

19. Chase Jr MW, Davies CA, Downey Jr JR, Frurip DJ, McDonald RA, Syverud AN (1985) JANAF thermochemical tables, 3rd ed. Natl Bureau of Standards, Washington, DC
20. Wash AD (1953) J Chem Soc 2266–2288
21. Dewar MJS, Ritchie JP, Alster J (1985) J Org Chem 50:1031–1036
22. O'Neal HE, Benson SW (1970) Kinetic data on gas phase unimolecular reactions. NSRDS-NB521, Washington, DC
23. Wodtke AM, Hintsa EJ, Lee YT (1986) J Phys Chem 90:3549–3558
24. McKee ML (1989) J Phys Chem 93:7365–7369
25. Saxon RP, Yoshimine M (1992) Can J Chem 70:572–578
26. Saxon RP, Yoshimine M (1989) J Phys Chem 93:3130–3135